AIP | The Journal of Chemical Physics

Density relaxation and particle motion characteristics in a non-ionic deep eutectic solvent (acetamide + urea): Time-resolved fluorescence measurements and all-atom molecular dynamics simulations

Anuradha Das, Suman Das, and Ranjit Biswas

Citation: The Journal of Chemical Physics **142**, 034505 (2015); doi: 10.1063/1.4906119
View online: http://dx.doi.org/10.1063/1.4906119
View Table of Contents: http://scitation.aip.org/content/aip/journal/jcp/142/3?ver=pdfcov
Published by the AIP Publishing

Density relaxation and particle motion characteristics in a non-ionic deep eutectic solvent (acetamide + urea): Time-resolved fluorescence measurements and all-atom molecular dynamics simulations

Anuradha Das, Suman Das, and Ranjit Biswas[a)]
Chemical, Biological and Macromolecular Sciences, S. N. Bose National Centre for Basic Sciences, Block-JD, Sector-III, Salt Lake, Kolkata, West Bengal 700098, India

(Received 25 October 2014; accepted 5 January 2015; published online 21 January 2015)

Temperature dependent relaxation dynamics, particle motion characteristics, and heterogeneity aspects of deep eutectic solvents (DESs) made of acetamide (CH_3CONH_2) and urea (NH_2CONH_2) have been investigated by employing time-resolved fluorescence measurements and all-atom molecular dynamics simulations. Three different compositions (f) for the mixture [$f CH_3CONH_2 + (1 - f)NH_2CONH_2$] have been studied in a temperature range of 328-353 K which is ~120-145 K above the measured glass transition temperatures (~207 K) of these DESs but much lower than the individual melting temperature of either of the constituents. Steady state fluorescence emission measurements using probe solutes with sharply different lifetimes do not indicate any dependence on excitation wavelength in these metastable molten systems. Time-resolved fluorescence anisotropy measurements reveal near-hydrodynamic coupling between medium viscosity and rotation of a dissolved dipolar solute. Stokes shift dynamics have been found to be too fast to be detected by the time-resolution (~70 ps) employed, suggesting extremely rapid medium polarization relaxation. All-atom simulations reveal Gaussian distribution for particle displacements and van Hove correlations, and significant overlap between non-Gaussian (α_2) and new non-Gaussian (γ) heterogeneity parameters. In addition, no stretched exponential relaxations have been detected in the simulated wavenumber dependent acetamide dynamic structure factors. All these results are in sharp contrast to earlier observations for ionic deep eutectics with acetamide [Guchhait *et al.*, J. Chem. Phys. **140**, 104514 (2014)] and suggest a fundamental difference in interaction and dynamics between ionic and non-ionic deep eutectic solvent systems. © *2015 AIP Publishing LLC.* [http://dx.doi.org/10.1063/1.4906119]

I. INTRODUCTION

Deep eutectic solvents (DESs) are increasingly finding a variety of industrial and technological applications due to their exquisite solvent properties, economical viability, and easy synthetic accessibility.[1–5] The bio-degradable nature of these multi-component melts makes these non-aqueous melt mixtures as suitable candidates for green solvent engineering and sustainable media for biomass processing.[6–8] DESs are molten mixtures at temperatures much below than the individual melting temperatures (T_m) of the constituents and may contain both ionic and non-ionic species. Extensive H-bond interaction among the components is believed to be a reason for the observed depression of freezing points. Such multi-component mixtures, when they contain electrolytes, are termed as ionic DESs.[1–4] Non-ionic DESs, on the other hand, are composed of dipolar molecules and amphiphiles. DESs made of acetamide and urea are representative examples of the latter kind and constitute the subject of the present study. Note that although a few fast spectroscopic measurements combined with computer simulations have attempted to illustrate the solute-solvent coupling in and relaxation dynamics of several ionic DESs,[9–15] similar studies are yet to be carried out for non-ionic members, such as (acetamide + urea) DESs. Here, we investigate, via employing both time-resolved fluorescence measurements and molecular dynamics simulations, the density relaxation timescales of the DESs [$f CH_3CONH_2 + (1 - f)NH_2CONH_2$] and coupling between a dissolved solute and density fluctuations in them at three different compositions (f) for the temperature range of 328–353 K.

The reasons that motivated us to take up the present study are as follows: First, pulsed field gradient nuclear magnetic resonance (PFG-NMR) measurements of DES made of choline chloride ($[HOC_2H_4N(CH_3)_3]^+ Cl^-$) and urea have suggested particle diffusion via jumps rather than through stochastic Brownian moves.[16] Interestingly, support for the presence of such a non-hydrodynamic transport mode for mixture components has been provided also by time-resolved fluorescence measurements of (acetamide + electrolyte) DESs which reported fractional viscosity dependence of average rotation and solvation rates ($\langle \tau_{r/s}^{-1} \rangle \propto \eta^{-p}$, $p < 1$) of a solute dissolved in them.[10–12,15] In such a situation, one would be naturally curious to know how density relaxes in deep eutectics made of acetamide and urea. As individual components, both acetamide and urea possess tremendous industrial and biological relevance. For example, molten acetamide (T_m ~ 353 K[17]) is known to solubilise a large number of organic and

[a)]Author to whom correspondence should be addressed. Electronic mail: ranjit@bose.res.in. Telephone: +91 33 2335 5706. Fax: +91 33 2335 3477.

inorganic compounds except cellulose, and may be utilised as a simple model system for understanding the role of hydrogen bonding interactions in determining the three dimensional structure of proteins and nucleic acids.[17–19]

Urea is, on the other hand, one of the most commonly used nitrogenous fertilizers and is known to critically impact protein stability and function.[20–24] Although the T_m of urea is ~406 K (acetamide + urea) exhibits a eutectic temperature of ~319 K at 0.62 mole fraction of acetamide.[25,26] This makes (acetamide + urea) DESs accessible for studying structure and dynamics in molten condition at a temperature range much lower than the individual T_ms of the components but more than 100 K above the thermodynamic glass transition temperature (T_g ~ 207 K) of the corresponding DES. This fact assumes even more importance as signatures of pronounced dynamic heterogeneity have been observed earlier[10–13] for (acetamide + electrolyte) DESs at a temperature of ~100-150 K above the corresponding T_gs. Apart from this basic scientific aspect, a smart application of (acetamide + urea) DESs as designer solvents for tailoring chemical reactions necessitates a thorough understanding of structure-dynamics relationship for these media. Here, the importance stems from the well-known solvent control of chemical reactions.[27–33] Interestingly, acetamide and urea, though can act as both H-bond donors and acceptors, possess vastly different molecular properties. For example, while the static dielectric constant (ε_0) of acetamide is ~60 and molecular dipole moment (μ) 3.2 D,[34,35] those values for urea are ~3 (measured in solid state) and 4.56 D,[36] respectively. Besides forming inter-species H-bonding, urea and acetamide also support intra-species H-bonding, leading to formation of dimers at low concentrations and polymers at high concentrations.[37,38] Given that the collective H-bonding network and polarity critically influences solvation timescales,[39–45] alteration of composition mixture provides an easy handle to regulate medium effects on a chemical reaction occurring in these media. Presence of polymeric as well as inter-species H-bonded molecules may give rise to medium heterogeneity sustaining slow dynamics in these systems.[46] More importantly, creation of liquid phase via extensive depression of freezing points of the mixture components may lead to microscopic heterogeneity in structure and dynamics of such media. These complexities of (acetamide + urea) DESs have been explored here via time-resolved fluorescence measurements of solute-centred dynamics and atomistic simulations of density relaxation and displacement distribution profiles.

II. EXPERIMENTAL DETAILS

A. Sample preparation

Coumarin 153 (C153) was used as received (exciton). *Trans*-2-[4-(dimethylamino)styryl]benzothiazole (DMASBT), a fluorescence probe with much shorter excited state average lifetime[12,47] than that of C153, was used (as received[48]) for an investigation of solution spatial heterogeneity via monitoring the excitation wavelength ($\lambda_{exc.}$) dependence of fluorescence emission of dissolved DMASBT. Acetamide (≥ 99%, SRL, India) and urea (>99%, SRL, India) were dried (~300 K) under mild vacuum overnight before use.

Samples were prepared by following the method described in detail elsewhere.[9–12,14,15] In brief, the required amount of DES components was mixed together in volumetric flasks, sealed, and heated using a hot water bath at a temperature of around ~355 K (Julabo, model F32) until the mixtures became completely molten. An aliquot of a given molten DESs was then quickly transferred into a pre-heated quartz cuvette (1 cm path length) which was pre-stained with dye (C153/DMASBT) grains and sealed. A few drops of (dye + hexane) solution was used for this "dye-staining," followed by removal of the career solvent (hexane) by gently blowing mild-hot air through the cuvette. Subsequently, the cuvette containing the sample and dye was brought near the experimental temperature via using a water-bath. Care was taken to ensure complete dissolution of the probe into the DES sample, maintain a dye (C153/DMASBT) concentration of $\leq 10^{-5}$ M in the solution under investigation. Spectral data were recorded after allowing the sample for about half-an-hour to equilibrate with pre-heated sample chamber at a designated temperature (328 K–353 K at an interval of 5 K). A few samples were bubbled with dry N_2 gas before data collection but did not produce any difference in data with those collected with the unbubbled samples.

B. Data collection and analyses for absorption, steady state and time resolved fluorescence studies

Steady state absorption spectra and fluorescence spectra were collected with a UV-visible spectrophotometer (UV-2450, Shimadzu) and a Fluoromax-3, Jobin-Yvon (Horiba) fluorimeter, respectively. Time correlated single photon counting (TCSPC) based set-up was used as before[10–12] (LifeSpec-ps, Edinburgh Instruments) for time-resolved fluorescence measurements which produced a pulse-width (full-width-at-half-maximum) of ~70 ps when an aqueous solution of non-dairy creamer was used as a scattering medium at the excitation wavelength of 409 nm. For measurements using C153, we used 409 nm light for excitation. Steady state spectroscopic data were then processed and analysed by following the method described elsewhere.[49–53]

Time resolved fluorescence anisotropy (r(t)) measurements were performed via following the standard protocol.[54–56] An iterative reconvolution algorithm[57] was used to simultaneously fit the collected parallel (I_{para}) and perpendicular (I_{perp}) decays. The geometric factor (G) was obtained via tail matching and found to be 1.15 ± 0.1. Dynamic anisotropic decays thus obtained were found to fit to bi-exponential functions of time, and the average rotation times ($\langle\tau_r\rangle$) were then obtained via time-integration, $\langle\tau_r\rangle = \int_0^\infty dt\ [r(t)/r(0)] = \int_0^\infty dt \sum_{i=1}^2 a_i \exp(t/\tau_i)$, with $\sum_i a_i = 1$ and the initial anisotropy, $r(0) = 0.376$ for C153.[54] Note here that Stokes shift dynamics[45] in these DESs were found to be too fast to be detected by the present set-up. However, magnitudes of dynamic Stokes shifts for C153 were estimated[58] using steady state absorption and emission spectra. Density, viscosity, and glass transition temperature (T_g) for these systems were measured by following the procedures described elsewhere.[14] While Table

S1 (supplementary material)[59] summarizes the composition dependent density and viscosity values for the temperature range considered, Fig. S1 provides a representative scan obtained from differential scanning calorimetric measurements of T_g for these DESs.

C. Simulation details

All-atom molecular dynamics simulations were performed with a total of 512 number of particles for (acetamide + urea) DESs for 0.6 and 0.7 acetamide mole fractions at 338 K employing GROMACS version 4.5.4,[60] where the molecules interacted via the following potential:

$$U(R) = \sum_{\text{bonds}} K_r(r-r_{eq})^2 + \sum_{\text{angles}} K_\theta(\theta-\theta_{eq})^2 + \sum_{\text{dihedrals}} K_\varphi(1+\cos(n\varphi-\delta)) + \sum_{i<j}^{\text{atoms}} \left(\frac{A_{ij}}{R_{ij}^{12}} - \frac{B_{ij}}{R_{ij}^{6}}\right) + \sum_{i<j}^{\text{atoms}} \frac{q_i q_j}{4\pi\varepsilon_0 R_{ij}}. \quad (1)$$

Note that the above generalized form of potential function has been used also for simulations of ionic liquids and found to provide reasonable description of liquid structure and dynamics.[61–70] In Eq. (1), K_r denotes the bond constant with the equilibrium bond distance r_{eq}, K_θ the angle constant with the equilibrium angle θ_{eq}, and K_φ the dihedral constant with periodicity n, dihedral angle ϕ, and phase shift δ. R_{ij} is the distance between i and j atoms with partial charges q_i and q_j, respectively. CHARMM[71] force field parameters were used for acetamide and GROMOS96 force field parameters for urea.[72] These force field parameters were found to generate simulation results that were in reasonable agreement with experiments for acetamide[10,11] and urea[72] in solutions. The short-range van der Waals interaction was represented by the Lennard-Jones (LJ) potential, and the long-range electrostatic potential was treated via particle mesh Ewald summation technique (PME).[73]

The initial configuration was built using Packmol[74] and minimized via the steepest decent algorithm in GROMACS. The H-bonds of the acetamide and urea molecules were kept constrained by applying the shake[75] algorithm with tolerance value of 10^{-4}. Then, each system was heated slowly from 100 K to 200 K and finally to 338 K with each step continuing for 100 ps in NVT ensemble. The final configuration was equilibrated in NPT ensemble at 1 atm pressure using Berendsen temperature and pressure coupling[76] with relaxation times of 0.5 ps and 2.0 ps, respectively, for 1 ns. Subsequently, further equilibration of 2 ns followed by a production run of 20 ns was carried out in NVT ensemble using Nose-Hoover thermostat.[77,78] Densities at 338 K in our simulations were found to be 1.12 gm/cc at 0.6 and 1.10 gm/cc at 0.7 acetamide mole fractions which agree well with the respective experimental densities (shown later). Periodic boundary conditions were employed in all three directions, and the equations of motion were integrated using a time step of 0.5 fs employing the leap-frog algorithm.[79] Simulated trajectories were saved every 0.1 ps for data analyses and simulation results.

III. RESULTS AND DISCUSSION

A. Spectroscopic measurements

1. Steady state spectral characteristics

Steady state absorption and emission spectra of C153 in these DESs at different compositions (at a fixed temperature) and temperatures (at a fixed composition) are presented in Figs. S2 and S3,[59] which indicate a near-invariance with both mixture composition and temperature. A more clear representation of this insensitivity (within ± 100 cm^{-1}) is provided in Fig. 1 where the absorption and emission spectral peak frequencies, and widths (full-width-at-half-maxima)[80,81] are shown as a function of temperature. Although these measurements are done within a narrow composition range, the observed spectral insensitivity is probably reflecting preferential solvation of dissolved C153 by the more polar component (ε_0 of acetamide and urea are ~60 and ~3, respectively) in the solution mixture. A more interesting aspect here is the temperature-independence of the spectral frequencies because temperature is known to frustrate the static correlations at the collective (that is, long wavelength) limit and hence reduce ε_0.[82–84] Note, however, that these spectral characteristics (frequencies and widths) are similar in magnitudes to those obtained for C153 in (acetamide + electrolyte) DESs[10,12] as acetamide has been the dominant component in all these melt mixtures.

We next explore the presence of spatial heterogeneity in these (acetamide + urea) DESs as $\lambda_{exc.}$ dependent fluorescence

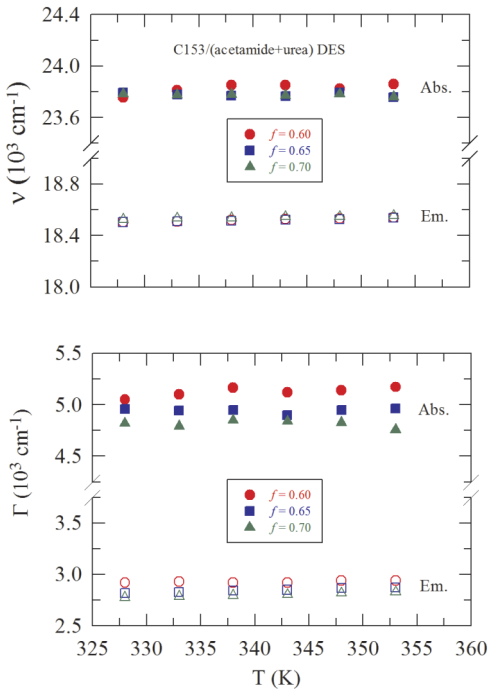

FIG. 1. Temperature dependent spectral characteristics of C153 in $[f CH_3CONH_2 + (1-f)NH_2CONH_2]$ DESs at three different acetamide mole fractions (f). Upper panel shows the variation of peak frequency (ν) and lower panel presents the variation in spectral width (Γ, full width at half maximum) of absorption (filled symbols) and emission spectra (open symbols) of C153 in these DESs at f = 0.6 (circles), 0.65 (squares), and 0.7 (triangles).

emission measurements (of a dissolved probe) of (acetamide + electrolyte) DES[10,12] have revealed inhomogeneous solution state. Probe dependence of the extent of emission shift induced by $\lambda_{exc.}$ observed there suggests the presence of domains with a distribution of relaxation times. As a competition between domain relaxation and probe's average excited state lifetime (τ_{life}) critically controls the detection of spatial heterogeneity through $\lambda_{exc.}$ dependence, we have employed two fluorescent probes (C153 and DMASBT) with sharply different τ_{life} (~5 ns for C153[45] and ~0.5 ns for DMASBT[12,47]) for our $\lambda_{exc.}$ dependent study of these DESs. Representative results are summarized in Fig. 2 where a change in $\lambda_{exc.}$ by ~120 nm (see Fig. S4 for the chosen $\lambda_{exc.}$ across the absorption spectra of these probes[59]) produces a variation of only ~100 cm^{-1} in the emission peak frequencies and widths for both these probes. Interestingly, a much larger variation in these spectral properties was observed earlier for ($CH_3CONH_2 + LiNO_3/Br/ClO_4$) DESs and attributed to the presence of spatial heterogeneity of solution structure.[85,86] Given the spectral resolution of our measurements (±200 cm^{-1}), a variation of only 100 cm^{-1} suggests that the associated density relaxation timescales are much faster than τ_{life} of these probes, making these systems to appear as "homogeneous" within the lifetime of these probes.

2. Time-resolved fluorescence measurements

As already shown,[10–12,87] fractional viscosity dependence of average solvation and rotation times measured via time-resolved fluorescence measurements may indicate the presence of temporal (or dynamic) heterogeneity in a given medium. Since solvation dynamics are too fast to be detected by the present set-up, we can provide only the estimated magnitudes of dynamic Stokes shift for C153 in these systems. Table S5[59] summarizes the estimated shift values at three different compositions for the temperature range of 328-353 K. Note in this table that the estimated shift values are within the range of ~750-900 cm^{-1}, which is similar to those reported[10] for (amide + electrolyte) DESs at higher temperatures. Although hydrodynamics predict the presence of a nanosecond diffusive timescale in these systems ($\sigma^2/D_T \approx 1$ ns at ~330 K for a particle of diameter, $\sigma \sim 4$ Å, diffusing through a medium with viscosity, $\eta \sim 10$ cP), it is interesting to note the absence of such a slow component in the present measurements. This is in contrast to our earlier findings for (amide + electrolyte) systems,[10,12,14,15] and may arise due to the extensive participation of the collective H-bond network of the present DESs and other fast modes[39–42] to the solvation process. Suitable dielectric relaxation measurements and simulations of density relaxations are required to understand the origin of such fast solvation response in these systems.

Rotational relaxation of the same dissolved solute is, however, much slower and can be detected in our experiments. Fig. 3 provides a representative example where collected r(t) decays at two different temperatures for C153 in the present DES at 0.6 acetamide mole fraction are shown. As indicated by dynamic Stokes shift measurements, these and other anisotropy decays collected at different compositions and temperatures contain a component much faster than the time-resolution (~70 ps) of our set-up and are bi-exponential functions of time. Reasonable bi-exponential description of all the collected r(t) decays has been found after constraining the faster time constant to 15 ps whose amplitude, depending upon composition and temperature, varies between ~25% and 75%. The rest is constituted by a slower component with time constant in 100-300 ps range (see Table S6).[59] Subsequently, the coupling between the solute rotation and the medium viscosity is explored in Fig. 4 where the logarithm of average rotation times measured at all the compositions and temperatures considered are shown as a function of logarithm of temperature-reduce viscosity. For a comparison, hydrodynamic slip predictions for rotation times of C153, with its shape factor incorporated,[54] in these DESs are also shown in the same figure. The increase of the measured average rotation times ($\langle\tau_r\rangle$) with viscosity can be described by an

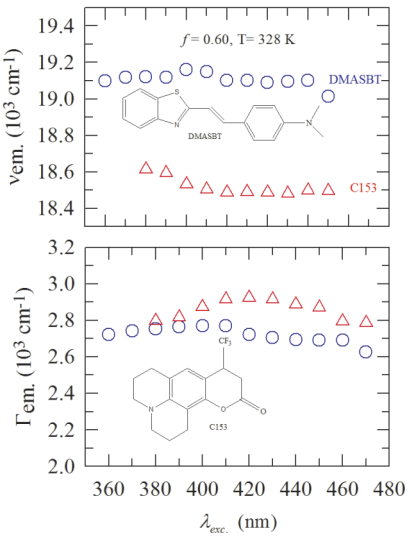

FIG. 2. Excitation wavelength ($\lambda_{exc.}$) dependence of fluorescence emission peak frequencies, ν_{em} (upper panel), and full-width-at-half-maxima, Γ_{em} (lower panel) for DMASBT (circles) and C153 (triangles) in [$f CH_3CONH_2$ + $(1-f)NH_2CONH_2$] with $f = 0.6$ at ~328 K. Chemical structures of DMASBT and C153 are also shown as insets.

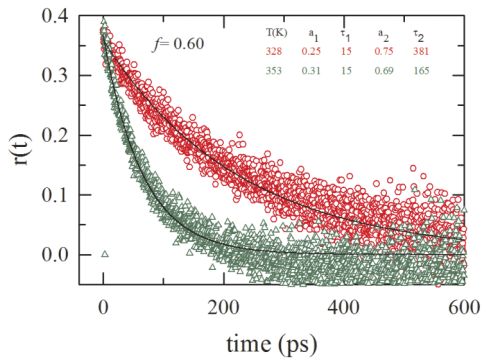

FIG. 3. Representative anisotropy decays at 328 K (red) and 353 K (green) for C153 in [$f CH_3CONH_2 + (1-f)NH_2CONH_2$] with $f = 0.6$. Circles denote the experimental data and solid lines fits through them. Fit parameters are shown in the inset. Time constants (τ_i) are in the unit of picoseconds. The goodness-of-fit parameters (χ^2) in these two temperatures are 1.06 and 1.09 for 328 and 353 K, respectively.

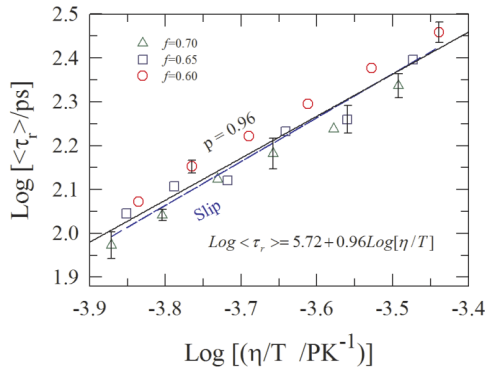

FIG. 4. Viscosity dependence of measured rotation times ($\langle\tau_r\rangle$) for C153 in $[f CH_3CONH_2+(1-f)NH_2CONH_2]$ at various temperatures, and comparison to hydrodynamic predictions using slip boundary condition (SBC). Measured rotation times are shown as a function of temperature-reduced viscosity (η/T) in a log-log fashion. Broken blue lines represent the hydrodynamic (Debye-Stokes-Einstein, DSE) predictions, $\tau_r^{DSE} = (V\eta/k_BT)fC$, with C153 volume V = 246 Å^3, shape factor (assuming ellipsoid) f = 1.71, and solute-solvent coupling parameter C = 0.24 (for SBC). Solid black line denotes the fit through the measured data. Stick predictions are much slower and thus not shown.

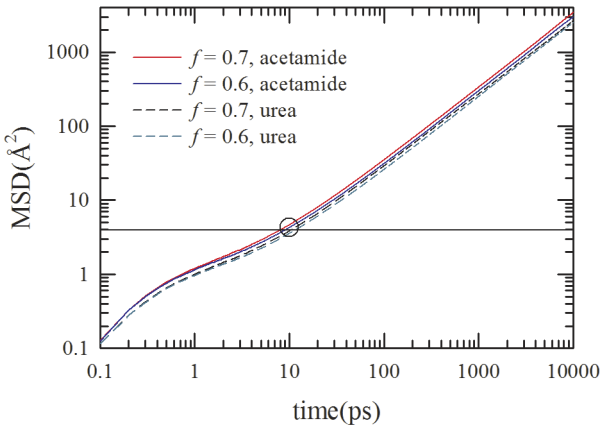

FIG. 5. Simulated MSDs for acetamide and urea in $[f CH_3CONH_2 + (1 - f)NH_2CONH_2]$ deep eutectics with $f = 0.6$ and 0.7 at 338 K. Solid lines represent MSDs for acetamide and broken lines for urea. Circle on MSD curves denote the simulated MSD values at 10 ps.

average linear fit which suggests a viscosity dependence of the following form: $\langle\tau_r\rangle \propto (\eta/T)^p$ with p = 0.96. The fraction power (p) maintained its value of near unity even when the measured $\langle\tau_r\rangle$ data were analysed separately (see Fig. S7).[59] Such a near-hydrodynamic viscosity dependence for average rotation times strongly suggests temporal homogeneity of the DESs under study, and it is in sharp contrast with our earlier findings for (amide + electrolyte) systems.[10,12,15] Arrhenius-type of temperature dependence for the average rotation rates ($(\langle\tau_r\rangle)^{-1}$) has been observed (see Fig. S8)[59] and the associated average activation energy (E_a) is found to be ~31.6 kJ mol^{-1}. Interestingly, a similar E_a has been found earlier for (CH_3CONH_2 + LiBr/NO_3) DESs[12] where pronounced heterogeneity characterized the solution structure and dynamics.

It is evident, therefore, that both the steady state and time-resolved fluorescence measurements of $[f CH_3CONH_2 + (1 - f)NH_2CONH_2]$ DESs using a dipolar solute suggest homogeneity in solution structure and dynamics. It would be instructive to learn, via simulations, whether such homogeneity is also preserved for the undoped system, that is, the DESs in the absence of any dipolar solute.

B. Simulation results

1. Mean-squared displacements (MSD): Search for cage-rattling

The simplest evidence for spatial heterogeneity due to domain formation arises from a time dependence of the MSD ($\langle|\Delta\mathbf{r}(t)|^2\rangle$) much weaker (that is, t^α with $\alpha < 1$) than that predicted in the Einstein's relation ($\langle|\Delta\mathbf{r}(t)|^2\rangle \propto t^1$)[88] even long after the inertial regime. This t^α dependence is a common occurrence in simulations of supercooled liquids, and interpreted as rattling motion of a particle confined in a cage formed by neighbours which are relaxing extremely slowly.[89] Signatures of rattling-in-a-cage motion have also been found in simulation studies of room temperatures ionic liquids[63,90] and ionic glasses.[91] Composition dependent MSDs at 338 K for both acetamide and urea, obtained from the simulated centre-of-mass position vectors ($\mathbf{r}^c(t)$) via the relation,[92] $\langle|\Delta\mathbf{r}(t)|^2\rangle = N^{-1}\langle\sum_{i=1}^{N}|\mathbf{r}_i^c(t) - \mathbf{r}_i^c(0)|^2\rangle$, are shown in Fig. 5. Note in this double logarithmic plot that there exists no indication of t^α dependence of the simulated MSDs other than the expected t^2 dependence at the initial inertial regime and t^1 dependence later in the diffusive regime. This behaviour of $\langle|\Delta\mathbf{r}(t)|^2\rangle$ is seen for high temperature bulk liquids[88,92] and liquid mixtures,[93] and suggests spatial homogeneity in solution structure. Simulated $\langle|\Delta\mathbf{r}(t)|^2\rangle$ presented here, therefore, supports the conclusion drawn from $\lambda_{exc.}$ dependence study (see Fig. 2) that these DESs are spatially homogenous. Simulated MSD curves are close to each other because of the narrow range of the composition considered. Interestingly, translational diffusion coefficients ($D_T = \left[\frac{\langle|\Delta\mathbf{r}(t)|^2\rangle}{6t}\right]_{t\to\infty}$) estimated from these MSDs for acetamide and urea are qualitatively similar to those obtained for these species in their respective aqueous solutions.[94,95]

2. Non-Gaussian (NG) parameters, van Hove functions, and displacement distributions: Search for dynamic heterogeneity

Time-resolved fluorescence anisotropy results presented in Fig. 4 have revealed near-hydrodynamic coupling between solute rotation and the viscosity of these DESs, and indicated that these DESs are, on an average, dynamically homogeneous. Since solute size plays a critical role for the observation of dynamic heterogeneity effects,[87,96] further investigation using microscopic tools is required to re-examine the above conclusion. A routine primary check for dynamic heterogeneity can be performed via the calculations of the NG[97] and new non-Gaussian (NNG)[98,99] parameters defined, respectively, as follows:

$$\alpha_2(t) = \frac{3\langle\delta r^4(t)\rangle}{5\langle\delta r^2(t)\rangle^2} - 1 \qquad (2)$$

and

$$\gamma(t) = \frac{1}{3}\left\langle \delta r^2(t)\right\rangle \left\langle \frac{1}{\delta r^2(t)}\right\rangle - 1, \tag{3}$$

with

$$\left\langle \frac{1}{\delta r^2(t)}\right\rangle = \left\langle \frac{1}{N}\sum_{i=1}^{N}\frac{1}{|\Delta \mathbf{r}_i(t)|^2}\right\rangle, \tag{4}$$

where $\left\langle \delta r^2(t)\right\rangle = \left\langle |\Delta \mathbf{r}(t)|^2\right\rangle$, and $\Delta \mathbf{r}_i(t) = \mathbf{r}_i^c(t) - \mathbf{r}_i^c(0)$ which denotes the displacement vector for the ith particle. Note NG ($\alpha_2(t)$) and NNG ($\gamma(t)$) parameters provide estimates of the slowest heterogeneity timescales in a given system and are associated with particle displacements, respectively, larger and smaller than those predicted by a Gaussian displacement distribution. For a system that do not possess dynamic heterogeneity, $\alpha_2(t)$ and $\gamma(t)$ curves are expected to significantly overlap with very similar peak times,[93] τ_{NG} and τ_{NNG}. In addition, the peak height of $\alpha_2(t)$ should be ~0.2 for such homogeneous systems.[89]

Fig. 6 presents a comparison between $\alpha_2(t)$ and $\gamma(t)$ simulated at 338 K for two different acetamide mole fractions. As discussed, both the curves overlap substantially with very similar peak heights (≤0.2) and peak times (~6-10 ps), indicating weak fluctuations in the local particle mobilities and near-homogeneous relaxation dynamics. Interestingly, the timescale of ~10 ps estimated for τ_{NG} and τ_{NNG} in these DESs corresponds to a mean displacement ($\sqrt{\left\langle |\Delta \mathbf{r}(t)|^2\right\rangle}$) of ~2 Å which is approximately half of the molecular diameter of an acetamide molecule.[12,15] In addition, $\left\langle |\Delta \mathbf{r}(t)|^2\right\rangle \propto t^1$ behaviour starts setting in around this timescale (see Fig. 5).

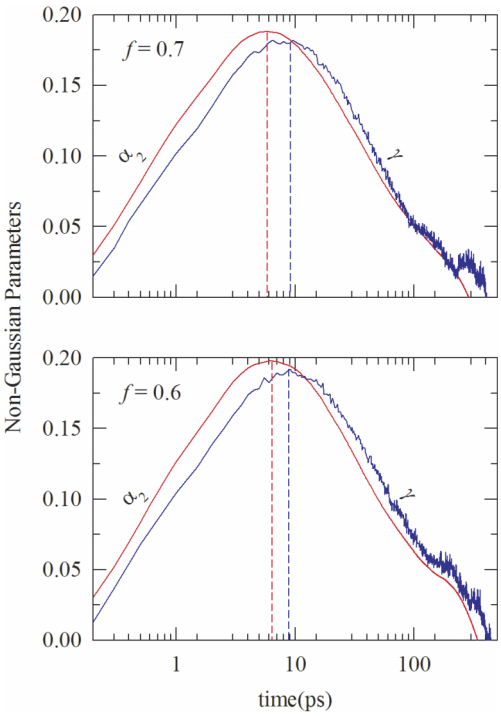

FIG. 6. Simulated non-Gaussian (α_2) and new non-Gaussian parameters for acetamide in [fCH$_3$CONH$_2$ + (1 − f)NH$_2$CONH$_2$] deep eutectics at 338 K. Vertical lines indicate the peak times (approximate), τ_{NG} and τ_{NNG}, discussed in the main text. Representations are color coded.

It would, therefore, be interesting to investigate the particle displacement distribution at this and longer timescales because diffusive dynamics are associated with the Gaussian distribution.[88] Note $\left\langle |\Delta \mathbf{r}(t)|^2\right\rangle \propto t^1$ behaviour does not necessarily guarantee a Gaussian displacement distribution,[46,62] and thus a closer look into the particle motion is necessary.

Next, we follow the self part of the van Hove correlation function, $G_s(\mathbf{r},t)$, for characterizing the particle motion which is defined as follows:[88]

$$G_s(\mathbf{r},t) = N^{-1}\left\langle \sum_{i=1}^{N}\delta\left[\mathbf{r}_i^c(t) - \mathbf{r}_i^c(0) - \mathbf{r}\right]\right\rangle, \tag{5}$$

whose Gaussian behaviour is described by the following relation:[63] $G_s^0(r,t) = [3/2\pi\left\langle |\Delta \mathbf{r}(t)|^2\right\rangle]^{3/2}\exp[-3r^2/(2\left\langle |\Delta \mathbf{r}(t)|^2\right\rangle)]$. $G_s(\mathbf{r},t)$ is connected to the single particle displacement distribution as follows:[98–101] $P[\log_{10}(\delta r);t] = \ln(10)4\pi\delta r^3 G_s(\delta r,t)$. For a Gaussian $G_s(\delta r,t)$, $P[\log_{10}(\delta r);t]$ attains a time-independent height of ~2.13.[98] Fig. 7 depicts the composition dependent simulated $G_s(\delta r,t)$ at four different times covering τ_{NNG} and other timescales deep into the diffusive regime. Corresponding particle displacement distributions, $P[\log_{10}(\delta r);t]$, are presented as insets of this figure. Calculated curves for Gaussian distributions are also shown for a comparison between simulated and calculated particle motion characteristics at these mixture compositions. It is evident that for both the compositions, the simulated van Hove correlation functions

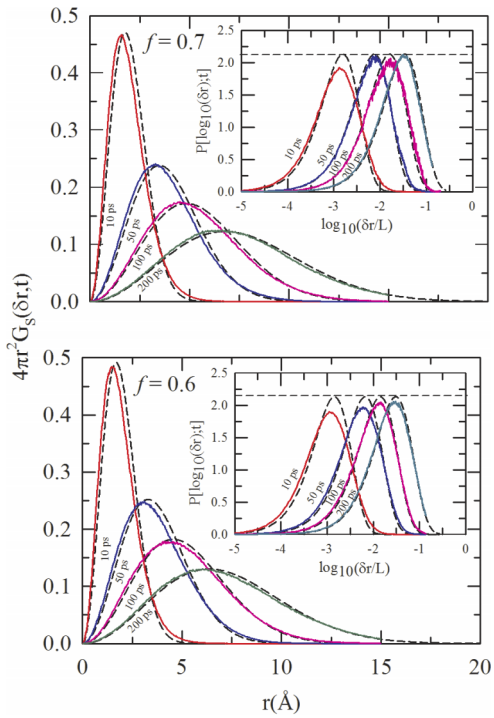

FIG. 7. Simulated self part of the van Hove correlation functions and particle displacement distributions for acetamide in [fCH$_3$CONH$_2$ + (1 − f)NH$_2$CONH$_2$] deep eutectics at 338 K at various times. Particle displacement distributions, $P[\log_{10}(\delta r);t]$, are shown as insets in which the abscissa is scaled by the respective simulation box lengths, L. These are 35.71 Å and 35.47 Å, respectively, at f = 0.7 and 0.6. van Hove correlations and particle displacement distributions obeying Gaussian statistics at those times are also shown (broken lines) for a comparison. Horizontal broken lines in each inset denote the peak height (2.13) for a Gaussian displacement distribution.

and displacement distributions deviate slightly at the earliest time (10 ps) but recover the Gaussian distribution. As time elapses, larger displacements are increasingly accessed at the cost of smaller moves, shifting the peak of $P[\log_{10}(\delta r);t]$ at longer distances but maintaining a peak-height destined by a Gaussian distribution. This further supports the view of over-all homogeneity in relaxation dynamics of these DESs and explains the near-hydrodynamic coupling between C153 rotation and medium viscosity reflected in Fig. 4.

3. Acetamide dynamic structure factor: Density relaxation profile and timescale

Next, we explore the density relaxation dynamics via simulating the self part of the acetamide dynamic structure factors, $F_s(k,t) = \langle \delta\rho_s(k,t)\delta\rho_s(-k,0)\rangle$, where $\delta\rho_s(k,t)$ denotes the wavenumber (k) and time dependent self part of the fluctuating acetamide density. The importance of following the decay kinetics of $F_s(k, t)$ stems from the fact that stretched exponential relaxation of relevant time correlation functions with stretching exponent (β) significantly less than unity is often considered as a signature of dynamic heterogeneity.[102,103] Fig. 8 presents the decay of normalized self dynamic structure factor, $F_s^N(k,t) = F_s(k,t)/F_s(k,t = 0)$, simulated at 338 K for acetamide at two different compositions along with the fits. The simulated decays correspond to the lowest wavenumber accessible to the present simulations ($k = 0.21$ Å^{-1}) and to the nearest neighbour wavenumber ($k = 1.34$ Å^{-1}). Fit parameters summarized in Table I clearly demonstrate the absence of any stretching exponent (β) less than unity. This is in contrast to strongly stretched exponential decay profiles of $F_s^N(k,t)$ for acetamide found earlier[10,11] in (acetamide + electrolyte) DESs which corroborated well with the fractional viscosity dependence of measured solute rotation rates in those systems. Therefore, the absence of fractional viscosity dependence in the measured solute rotation rates and stretching exponent in the simulated acetamide self dynamic structure factor strongly suggests absence of any dynamic heterogeneity in these (acetamide + urea) deep eutectics. Note that the $F_s^N(k,t)$ relaxations at $k = 1.34$ Å^{-1} possess a significant sub-picosecond component with average relaxation time ($\langle\tau\rangle$) below 10 ps. Such a fast nearest neighbour density relaxation explains absence of excitation wavelength dependence of fluorescence emission even for a shorter lifetime probe used in this study (see Fig. 2). Also, note that time constants associated with the slowest components of these nearest neighbour decays are quite close to heterogeneity timescales (τ_{NG} and τ_{NNG}), providing further support to the dynamical homogeneity view of these deep eutectics.

TABLE I. Multi-exponential fit parameters for simulated wavenumber dependent $F_s^N(k, t)$ for acetamide in (acetamide + urea) deep eutectics at 338 K and two acetamide mole fractions.

f	k (Å^{-1})	a_1	t_1 (ps)	a_2	t_2 (ps)	a_3	t_3 (ps)	β	$\langle\tau\rangle$ (ps)
0.7	0.21	1.0	416	...	...	...	...	1.0	416
0.7	1.34	0.25	0.46	0.16	4.1	0.59	12.82	1.0	8.3
0.6	0.21	1.0	476	...	...	...	...	1.0	476
0.6	1.34	0.25	0.49	0.19	5.26	0.56	14.93	1.0	9.5

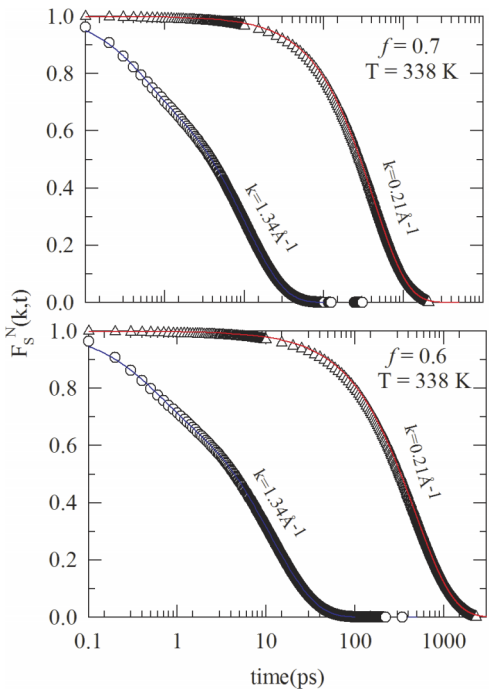

FIG. 8. Simulated wavenumber dependent relaxation of the normalized self part of the acetamide dynamic structure factor, $F_s^N(k, t)$, for $[f CH_3CONH_2 + (1 - f)NH_2CONH_2]$ deep eutectics at 338 K with $f = 0.7$ and 0.6. Multi-exponential fits through the simulated data are shown by solid lines. Fit parameters are summarized in Table I.

IV. CONCLUDING REMARKS

In conclusion, our combined time-resolved fluorescence and all-atom simulation study indicate that the (acetamide + urea) deep eutectics studied here are both spatially and dynamically homogeneous systems although these systems have been studied at a temperature range much lower than the individual melting temperatures of the constituents. This is in sharp contrast to earlier findings for (acetamide + electrolyte) deep eutectics and indicates qualitative difference between these two classes of deep eutectic systems. The interpretation of fluorescence results in terms of homogeneous solution structure and dynamics has been supported by the simulated mean squared displacement profiles, heterogeneity parameters, displacement distributions, particle motion characteristics, and relaxation of dynamic structure factors. Simulated particle displacements are found to be Gaussian and thus do not support existence of any non-hydrodynamic moves such as jumps. The observation that the Stokes shift dynamics in these DESs are too fast to be detected by the present measurements is supported by the simulated relaxation of acetamide dynamic structure factors which reports significant sub-picosecond relaxation component along with average relaxation time <10 ps. This is much faster than what was observed earlier for acetamide relaxation in the presence of electrolytes.[10,11]

The qualitative difference between these two classes of DESs may be understood by comparing the H-bond formation and dynamics[19] between these DESs. Study of low frequency collective dynamics employing Kerr spectroscopic measurements[19] and orientational motions via dielectric relaxation measurements of these systems can reveal important information on inter- and intra-species association of these systems. Development of semi-molecular theories for understanding the orientational relaxation and Stokes shift dynamics along the line of what has been done for binary mixtures of ionic liquids with common solvents[104–107] are required to provide microscopic understanding of relaxation dynamics of these exciting media. Smart applications of DESs as designer solvents demand such a robust knowledge.

ACKNOWLEDGMENTS

A.D. acknowledges UGC, India, and S.D. thanks CSIR, India, for providing research fellowships. Computational facilities availed through the TUE-CMS project (SR/NM/NS-29/2011(G)) at the centre is gratefully acknowledged.

[1]D. V. Wagle, H. Zhao, and G. A. Baker, Acc. Chem. Res. **47**, 2299 (2014).
[2]Q. Zhang, K. D. O. Vigier, S. Royer, and F. Jérôme, Chem. Soc. Rev. **41**, 7108 (2012).
[3]A. P. Abbott, G. Capper, D. L. Davies, R. K. Rasheed, and V. Tambyrajah, Chem. Commun. **2003**, 70.
[4]A. P. Abbott, D. Boothby, G. Capper, D. L. Davies, and R. K. Rasheed, J. Am. Chem. Soc. **126**, 9142 (2004).
[5]M. Francisco, A. Van Den Bruinhorst, and M. C. Kroon, Angew. Chem., Int. Ed. **52**, 3074 (2013).
[6]M. Francisco, A. Van Den Bruinhorst, and M. C. Kroon, Green Chem. **14**, 2153 (2012).
[7]H. Zhao and G. A. Baker, J. Chem. Technol. Biotechnol. **88**, 3 (2013).
[8]D. Carriazo, M. C. Serrano, M. C. Gutierrez, M. L. Ferrer, and F. del Monte, Chem. Soc. Rev. **41**, 4996 (2012).
[9]R. Biswas, A. Das, and H. Shirota, J. Chem. Phys. **141**, 134506 (2014).
[10]B. Guchhait, S. Das, S. Daschakraborty, and R. Biswas, J. Chem. Phys. **140**, 104514 (2014).
[11]A. Das, S. Das, and R. Biswas, Chem. Phys. Lett. **581**, 47 (2013).
[12]B. Guchhait, S. Daschakraborty, and R. Biswas, J. Chem. Phys. **136**, 174503 (2012).
[13]T. Pal and R. Biswas, Chem. Phys. Lett. **517**, 18 (2011).
[14]H. Gazi, B. Guchhait, S. Daschakraborty, and R. Biswas, Chem. Phys. Lett. **501**, 358 (2011).
[15]B. Guchhait, H. Gazi, H. K. Kashyap, and R. Biswas, J. Phys. Chem. B **114**, 5066 (2010).
[16]C. D'Agostino, R. C. Harris, A. P. Abbott, L. F. Gladden, and M. D. Mantle, Phys. Chem. Chem. Phys. **13**, 21383 (2011).
[17]D. H. Kerridge, Chem. Soc. Rev. **17**, 181 (1988).
[18]D. A. Dixon, K. D. Dobbs, and J. J. Valentini, J. Phys. Chem. **51**, 13435 (1994).
[19]S. Das, R. Biswas, and B. Mukherjee, "Reorientational jump dynamics and its connections to hydrogen bond relaxation in molten acetamide," J. Phys. Chem. B **119**, 274 (2015).
[20]L. Hua, R. Zhou, D. Thirumalai, and B. J. Berne, Proc. Natl. Acad. Sci. U. S. A. **105**, 16928 (2008).
[21]A. Das and C. Mukhopadhyay, J. Phys. Chem. B **113**, 12816 (2009).
[22]D. Bandyopadhyay, S. Mohan, S. K. Ghosh, and N. Choudhury, J. Phys. Chem. B **118**, 11757 (2014).
[23]L. B. Sagle, Y. Zhang, V. A. Litosh, X. Chen, Y. Cho, and P. S. Cremer, J. Am. Chem. Soc. **131**, 9304 (2009).
[24]B. J. Bennion and V. Daggett, Proc. Natl. Acad. Sci. U. S. A. **100**, 5142 (2003).
[25]L. Walbrugh, "Amitraj solid dosage form," M.S. thesis (University of Pretoria, Pretoria, South Africa, 2006).
[26]S. Rajkhowa, A. Das, S. Mahiuddin, and R. Biswas, J. Chem. Eng. Data **57**, 3467 (2012).
[27]G. van der Zwan and J. T. Hynes, Chem. Phys. **152**, 169 (1991).
[28]G. van der Zwan and J. T. Hynes, J. Chem. Phys. **78**, 4174 (1983).
[29]A. Nitzan, *Chemical Dynamics in Condensed Phases* (Oxford University Press, Oxford, 2006).
[30]T. Pradhan and R. Biswas, J. Phys. Chem. A **111**, 11524 (2007).
[31]T. Pradhan, H. A. R. Gazi, and R. Biswas, J. Chem. Phys. **131**, 054507 (2009).
[32]R. Biswas and B. Bagchi, J. Chem. Phys. **105**, 7543 (1996).
[33]R. K. Murarka, S. Bhattacharyya, R. Biswas, and B. Bagchi, J. Chem. Phys. **110**, 7365 (1999).
[34]O. F. Stafford, J. Am. Chem. Soc. **55**, 3987 (1933).
[35]R. Wallace, Inorg. Chem. **11**, 414 (1972).
[36]W. D. Kumler and G. M. Fohlen, J. Am. Chem. Soc. **64**, 1944 (1942).
[37]A. S. Mahadevi, Y. I. Neela, and G. N. Sastry, Phys. Chem. Chem. Phys. **13**, 15211 (2011).
[38]J. K. Carr, L. E. Buchanan, J. R. Schmidt, M. T. Zanni, and J. L. Skinner, J. Phys. Chem. B **117**, 13291 (2013).
[39]B. Bagchi and R. Biswas, Adv. Chem. Phys. **109**, 207 (1999).
[40]S. Roy and B. Bagchi, J. Chem. Phys. **99**, 1310 (1993).
[41]S. Roy and B. Bagchi, J. Chem. Phys. **99**, 9938 (1993).
[42]R. Biswas and B. Bagchi, J. Phys. Chem. B **100**, 1238 (1996).
[43]H. K. Kashyap, T. Pradhan, and R. Biswas, J. Chem. Phys. **125**, 174506 (2006).
[44]S. Daschakraborty, T. Pal, and R. Biswas, J. Chem. Phys. **139**, 164503 (2013).
[45]M. L. Horng, J. A. Gardecki, A. Papazyan, and M. Maroncelli, J. Phys. Chem. **99**, 17311 (1995).
[46]T. Pal and R. Biswas, J. Chem. Phys. **141**, 104501 (2014).
[47]M. Kondo, X. Li, and M. Maroncelli, J. Phys. Chem. B **117**, 12224 (2013).
[48]DMASBT was used as received as a gift from Professor Mark Maroncelli, Penn. State University, USA.
[49]T. Pradhan, P. Ghoshal, and R. Biswas, J. Phys. Chem. A **112**, 915 (2008).
[50]H. A. R. Gazi and R. Biswas, J. Phys. Chem. A **115**, 2447 (2011).
[51]R. Biswas, A. R. Das, T. Pradhan, D. Touraud, W. Kunz, and S. Mahiuddin, J. Phys. Chem. B **112**, 6620 (2008).
[52]B. Guchhait and R. Biswas, J. Chem. Phys. **138**, 114909 (2013).
[53]B. Guchhait, R. Biswas, and P. K. Ghorai, J. Phys. Chem. B **117**, 3345 (2013).
[54]M. L. Horng, J. A. Gardecki, and M. Maroncelli, J. Phys. Chem. A **101**, 1030 (1997).
[55]T. Pradhan, P. Ghoshal, and R. Biswas, J. Chem. Sci. **120**, 275 (2008).
[56]N. Sarma, J. M. Borah, S. Mahiuddin, H. A. R. Gazi, B. Guchhait, and R. Biswas, J. Phys. Chem. B **115**, 9040 (2011).
[57]A. J. Cross and G. R. Fleming, Biophys. J. **46**, 45 (1984).
[58]R. S. Fee and M. Maroncelli, Chem. Phys. **183**, 235 (1994).
[59]See supplementary material at http://dx.doi.org/10.1063/1.4906119 for composition dependent density and viscosity values for the temperature range of 328-353 K, a representative DSC scan showing T_g, absorption and emission spectra of C153 at various compositions (at a given temperature), and temperatures (at a given composition), estimated dynamic Stokes shifts for C153 at three different compositions, figure showing plots of measured $\langle\tau_r\rangle$ versus η/T at different acetamide mole fractions, and Arrhenius plots for measured $\langle\tau_r\rangle$.
[60]D. van der Spoel, E. Lindahl, B. Hess, A. R. van Buuren, E. Apol, P. J. Meulenhoff, D. P. Tieleman, A. L. T. M. Sijbers, K. A. Feenstra, R. van Drunen, and H. J. C. Berendsen, Gromacs User Manual version 4.5.4, www.gromacs.org (2010).
[61]J. Habasaki and K. Nagi, J. Chem. Phys. **129**, 194501 (2008).
[62]T. Pal and R. Biswas, Theor. Chem. Acc. **132**, 1348 (2013).
[63]M. G. Del Popolo and G. A. Voth, J. Phys. Chem. B **108**, 1744 (2004).
[64]T. I. Morrow and E. J. Maginn, J. Phys. Chem. B **106**, 12807 (2002).
[65]J. N. C. Lopes, J. Deschamps, and A. A. H. Padua, J. Phys. Chem. B **108**, 2038 (2004).
[66]C. G. Hanke, S. L. Price, and R. M. Lynden-Bell, Mol. Phys. **99**, 801 (2001).
[67]C. J. Margulis, Mol. Phys. **102**, 829 (2004).
[68]X. P. Wu, Z. P. Liu, S. P. Huang, and W. C. Wang, Phys. Chem. Chem. Phys. **7**, 2771 (2005).
[69]D. Roy and M. Maroncelli, J. Phys. Chem. B **114**, 12629 (2010).
[70]B. L. Bhargava and S. Balasubramanian, J. Chem. Phys. **123**, 144505 (2005).
[71]A. D. Mackerell, Jr., J. Wiorkiewicz-Kuczera, and M. Karplus, J. Am. Chem. Soc. **117**, 11946 (1995).
[72]L. J. Smith, H. J. C. Berendsen, and W. F. Van Gunsteren, J. Phys. Chem. B **108**, 1065 (2004).

[73]U. Essmann, L. Perera, M. L. Berkowitz, T. Darden, H. Lee, and L. G. Pedersen, J. Chem. Phys. **103**, 8577 (1995).
[74]L. Martinez, R. Andrade, E. G. Birgin, and J. M. Martinez, J. Comput. Chem. **30**, 2157 (2009).
[75]J. P. Ryckaert, G. Ciccotti, and H. J. C. Berendsen, J. Comput. Phys. **23**, 327 (1977).
[76]H. J. C. Berendsen, J. P. M. Postma, W. F. van Gunsteren, A. DiNola, and J. R. Haak, J. Chem. Phys. **81**, 3684 (1984).
[77]S. Nose, Mol. Phys. **52**, 255 (1984).
[78]W. G. Hoover, Phys. Rev. A **31**, 1695 (1985).
[79]R. W. Hockney, S. P. Goel, and J. Eastwood, J. Comput. Phys. **14**, 148 (1974).
[80]R. Biswas, J. E. Lewis, and M. Maroncelli, Chem. Phys. Lett. **310**, 485 (1999).
[81]J. E. Lewis, R. Biswas, A. G. Robinson, and M. Maroncelli, J. Phys. Chem. B **105**, 3306 (2001).
[82]C. Ronne, L. Thrane, P.-O. Astrand, A. Wallqvist, K. V. Mikkelsen, and S. O. Keiding, J. Chem. Phys. **107**, 5319 (1997).
[83]M. Petrowosky and R. Frech, J. Phys. Chem. B **113**, 16118 (2009).
[84]J. Hunger, A. Stoppa, S. Schrodle, G. Hefter, and R. Buchner, ChemPhysChem **10**, 723 (2009).
[85]P. K. Mandal, M. Sarkar, and A. Samanta, J. Phys. Chem. A **108**, 9048 (2004).
[86]Z. Hu and C. J. Margulis, Proc. Natl. Acad. Sci. U. S. A. **103**, 831 (2006).
[87]M. D. Ediger, Annu. Rev. Phys. Chem. **51**, 99 (2000).
[88]J. P. Hansen and I. R. McDonald, *Theory of Simple Liquids*, 3rd ed. (Academic, San Diego, 2006).
[89]F. Faupel, W. Frank, M.-P. Macht, H. Mehrer, V. Naundorf, K. Ratzke, H. R. Schober *et al.*, Rev. Mod. Phys. **75**, 237 (2003).
[90]D. Roy, N. Patel, S. Conte, and M. Maroncelli, J. Phys. Chem. B **114**, 8410 (2010).
[91]J. Habasaki and K. L. Ngai, J. Non-Cryst. Solids **352**, 5170 (2006).
[92]M. P. Allen and D. J. Tildeseley, *Computer Simulations of Liquids* (Oxford University Press, New York, 1987).
[93]S. Indra and R. Biswas, "Hydrogen-bond dynamics of water in presence of an amphiphile, tetramethylurea: Signature of confinement-induced effects," Mol. Simul. (published online).
[94]H. J. Christoffers and G. Kegeles, J. Am. Chem. Soc. **85**, 2562 (1963).
[95]A. Idrissi, S. Sokolić, and A. Perera, J. Chem. Phys. **112**, 9479 (2000).
[96]W. Huang and R. Richert, Philos. Mag. **87**, 371 (2007).
[97]A. Rahman, Phys. Rev. **136**, 405 (1964).
[98]E. Flenner and G. Szamel, Phys. Rev. E **72**, 011205 (2005).
[99]K. Kim and S. Saito, J. Chem. Phys. **133**, 044511 (2010).
[100]D. R. Reichman, E. Rabani, and P. L. Geissler, J. Phys. Chem. B **109**, 14654 (2005).
[101]A. M. Puertas, M. Fuchs, and M. E. Cates, J. Chem. Phys. **121**, 2813 (2004).
[102]C. A. Angell, K. L. Ngai, G. B. McKenna, P. F. McMillan, and S. W. Martin, J. Appl. Phys. **88**, 3113 (2000).
[103]D. A. Turton, J. Hunger, A. Stoppa, G. Hefter, A. Thoman, M. Walther, R. Buchner, and K. Wynne, J. Am. Chem. Soc. **131**, 11140 (2009).
[104]T. Pal and R. Biswas, J. Chem. Phys. **141**, 164502 (2014).
[105]S. Daschakraborty and R. Biswas, J. Phys. Chem. B **118**, 1327 (2014).
[106]S. Daschakraborty and R. Biswas, J. Phys. Chem. B **115**, 4011 (2011).
[107]S. Daschakraborty and R. Biswas, J. Chem. Phys. **140**, 014504 (2014).